arXiv:1211.1112v4 [hep-ph] 1 May 2013

KU-PH-013
TTP12-042
SFB/CPP-12-85

Full $\mathcal{O}(\alpha)$ electroweak radiative corrections to $e^+e^- \to t\bar{t}\gamma$ with GRACE-Loop

P.H. Khiem[A,B], J. Fujimoto[A], T. Ishikawa[A], T. Kaneko[A],
K. Kato[C], Y. Kurihara[A],
Y. Shimizu[A], T. Ueda[D], J.A.M. Vermaseren[E], Y. Yasui[F]

[A)] *KEK, Oho 1-1, Tsukuba, Ibaraki 305-0801, Japan.*
[B)] *SOKENDAI University, Shonan Village, Hayama, Kanagawa 240-0193 Japan.*
[C)] *Kogakuin University, Shinjuku, Tokyo 163-8677, Japan.*
[D)] *Karlsruhe Institute of Technology (KIT), D-76128 Karlsruhe, Germany.*
[E)] *NIKHEF, Science Park 105, 1098 XG Amsterdam, The Netherlands.*
[F)] *Tokyo Management College, Ichikawa, Chiba 272-0001, Japan.*

Abstract

We present the full $\mathcal{O}(\alpha)$ electroweak radiative corrections to the process $e^+e^- \to t\bar{t}\gamma$ at the International Linear Collider (ILC). The computation is performed with the help of the GRACE-Loop system. We present the total cross-section and the top quark forward-backward asymmetry (A_{FB}) as a function of the center-of-mass energy and compare them with the process $e^+e^- \to t\bar{t}$. We find that the value of A_{FB} in $t\bar{t}\gamma$ production is larger than A_{FB} in $t\bar{t}$ production. It is an important result for the measurement of the top quark forward-backward asymmetry at the ILC. Applying a structure function method, we also subtract the QED correction to gain the genuine weak correction in both the α scheme and the G_μ scheme ($\delta_W^{G_\mu}$). We obtain numerical values for $\delta_W^{G_\mu}$ which are changing from 2% to -24% when we vary the center-of-mass energy from 360 GeV to 1 TeV.

1 Introduction

The experimental results of CDF [1] and D0 [2] on the measurement of top pair production at the Tevatron show an unexpected large top quark forward-backward asymmetry. The precise theoretical calculations of the top pair production play an important role in explaining the experimental data. QCD radiative corrections to top pair production from proton-proton collisions were calculated by several authors [3], [4], [5], [6], [7]. However, the measurement is affected by a huge background from QCD. A good example is the $gg \to t\bar{t}$ reaction. In the future, the measurement will be performed at the ILC without QCD background. Therefore, we consider the precise calculations of top pair production and top pair with photon production in e^+e^- collisions. A completed full one-loop electroweak correction calculation to the process $e^+e^- \to t\bar{t}$ has already been presented in refs [8], [9], [10]. In this paper, we calculate the full $\mathcal{O}(\alpha)$ electroweak radiative corrections to both the process $e^+e^- \to t\bar{t}$ and $e^+e^- \to t\bar{t}\gamma$ at the ILC.

The data of the ATLAS [11] and CMS [12] experiments prove the existence of a new boson with mass around 126GeV. It is assumed to be the standard-model Higgs particle. Once the discovery of the Higgs boson is confirmed, the next important task is to measure its properties. However, it is clear that such a measurement is much easier at the cleaner environment of the ILC than at the LHC with its large QCD backgrounds. To measure the properties of the new boson it is important that also the radiative correction calculations for the ILC take the complete standard model into account.

The experiments at the ILC require a precise determination of the luminosity which will be based on higher order theoretical calculations of the Bhabha scattering cross-section. Thus, the computation of electroweak radiative corrections to the process $e^+e^- \to e^+e^-\gamma$ is mandatory. This will be our eventual target. However, as a first step, we are going to calculate the process $e^+e^- \to t\bar{t}\gamma$ which is easier in several respects: there are fewer diagrams and the numerical cancellations between the diagrams are less severe. It will provide a framework for our target calculation.

In the scope of this paper, we discuss the full $\mathcal{O}(\alpha)$ electroweak radiative corrections to the process $e^+e^- \to t\bar{t}\gamma$ at ILC. We then examine the numerical results of the top quark forward-backward asymmetry as well as the genuine weak corrections in both the α scheme and the G_μ scheme [13] as compared to the process $e^+e^- \to t\bar{t}$.

The paper is organized as follows. In section 2 we introduce the GRACE-Loop system and set up the calculation. In section 3 we discuss the numerical results of the calculation. Future plans and conclusions of our paper are presented in section 4.

2 GRACE-Loop and the process $e^-e^+ \to t\bar{t}\gamma$

2.1 GRACE-Loop

The computation is performed with the help of the GRACE-Loop system which is a generic program for the automatic calculation of scattering processes in High Energy Physics. Of course, with a system this complicated still under development, it is important to have as many tests as possible of the correctness of the answer. Hence the GRACE-Loop system has been equipped with non-linear gauge fixing terms in the Lagrangian which will be described in some of the next paragraphs. The renormalization has been carried out with the on-shell renormalization condition of the Kyoto scheme, as described in ref [14]. The program was presented and checked carefully with a variety of $2 \to 2$-body electroweak processes in ref [15]. The GRACE-Loop system has also been used to calculate $2 \to 3$-body processes such as $e^+e^- \to ZHH$ [16], $e^+e^- \to t\bar{t}H$ [17], $e^+e^- \to \nu\bar{\nu}H$ [18]. The above calculations have been done independently by other groups, for example the process $e^+e^- \to ZHH$ [19], $e^+e^- \to t\bar{t}H$ [20], [21], [22] and $e^+e^- \to \nu\bar{\nu}H$ [23], [24]. Moreover, the $2 \to 4$-body process as $e^+e^- \to \nu_\mu\bar{\nu}_\mu HH$ [25] was calculated successfully by GRACE-loop system.

The steps of calculating a process in the GRACE system are as follows. First the system requires input files that describe the Feynman rules of the model. In this case, we use the standard model. These files are considered part of the system but for different models the user would have to provide them. Next a (small) file is needed that selects the model, the names of the incoming and outgoing particles, and one of a set of predefined kinematic configurations for the phase space integration. In the intermediate stage symbolic manipulation handles all Dirac and tensor algebra in n-dimensions, reduces the formulas to coefficients of tensor one-loop integrals and writes the formulas in terms of FORTRAN subroutines on a diagram by diagram basis. For this manipulation either FORM [26] or REDUCE [27] is used. The FORTRAN routines will be combined with libraries which contain the routines that reduce the tensor one-loop integrals into scalar one-loop integrals. The scalar one-loop integrals will be numerically evaluated by one of the FF [28] or LoopTools [29] packages. The ultraviolet divergences (UV-divergences) are regulated by dimensional regularization and the infrared divergences (IR-divergences) will be regulated by giving the photon an infinitesimal mass λ. Eventually all FORTRAN routines are compiled and linked with the GRACE libraries which include the kinematic libraries and the Monte Carlo integration program BASES [30]. The resulting executable program can then calculate cross-sections and generate events.

Ref [15] describes the method used by the GRACE-Loop system to reduce the tensor one-loop five- and six-point functions into one-loop four-point functions.

The GRACE-Loop system allows the use of non-linear gauge fixing conditions [31]

which are defined by:

$$\begin{aligned}\mathcal{L}_{GF} &= -\frac{1}{\xi_W}|(\partial_\mu - ie\tilde{\alpha}A_\mu - igc_W\tilde{\beta}Z_\mu)W^{\mu+} + \xi_W\frac{g}{2}(v+\tilde{\delta}H+i\tilde{\kappa}\chi_3)\chi^+|^2 \\ &\quad -\frac{1}{2\xi_Z}(\partial\cdot Z + \xi_Z\frac{g}{2c_W}(v+\tilde{\varepsilon}H)\chi_3)^2 - \frac{1}{2\xi_A}(\partial\cdot A)^2 \ . \end{aligned} \tag{1}$$

We are working in the R_ξ-type gauges with condition $\xi_W = \xi_Z = \xi_A = 1$ (with so-called the 't Hooft-Feynman gauge), there is no contribution of the longitudinal term in the gauge propagator. This choice has not only the advantage of making the expressions much simpler. It also avoids unnecessary large cancellations, high tensor ranks in the one-loop integrals and extra powers of momenta in the denominators which cannot be handled by the FF package.

The GRACE-Loop system can also use an axial gauge for external photons. This has two advantages.

1. It cures a problem with large numerical cancellations. This is very useful when calculating the process at small angle and energy cuts of the final state particles.
2. It provides a useful tool to check the consistency of the results which, due to the Ward identities, must be independent of the choice of the gauge.

2.2 The numerical test of the process $e^-e^+ \to t\bar{t}\gamma$

The full set of Feynman diagrams with the non-linear gauge fixing as described before consists of 16 tree diagrams and 1704 one-loop diagrams (of which 168 are pentagon diagrams). In Fig 1 we show some selected diagrams.

The results are checked carefully by three kinds of consistency tests. These tests are performed with quadruple precision at a few random points in the phase space. The first test is ultraviolet finiteness of the results. This test is done on all virtual one-loop diagrams and their counter terms and we treat $C_{UV} = 1/\epsilon - \gamma_E + \log 4\pi$ as a parameter. In order to regularize the infrared divergences, we give the virtual photon a fictitious mass, $\lambda = 10^{-17}$GeV. In the table 1 we present the numerical results of the test at one random point in the phase space. The result is stable over more than 30 digits for various values of the ultraviolet parameter.

The second test is the independence of the result on the fictitious photon mass λ. In this case, we take $C_{UV} = 0$. This test will be performed by including as well the virtual loop diagrams as the soft bremsstrahlung contribution. In table 2 the numerical results of the test are presented. We find that the result is stable over more than 15 digits when varying the parameter λ over a wide range.

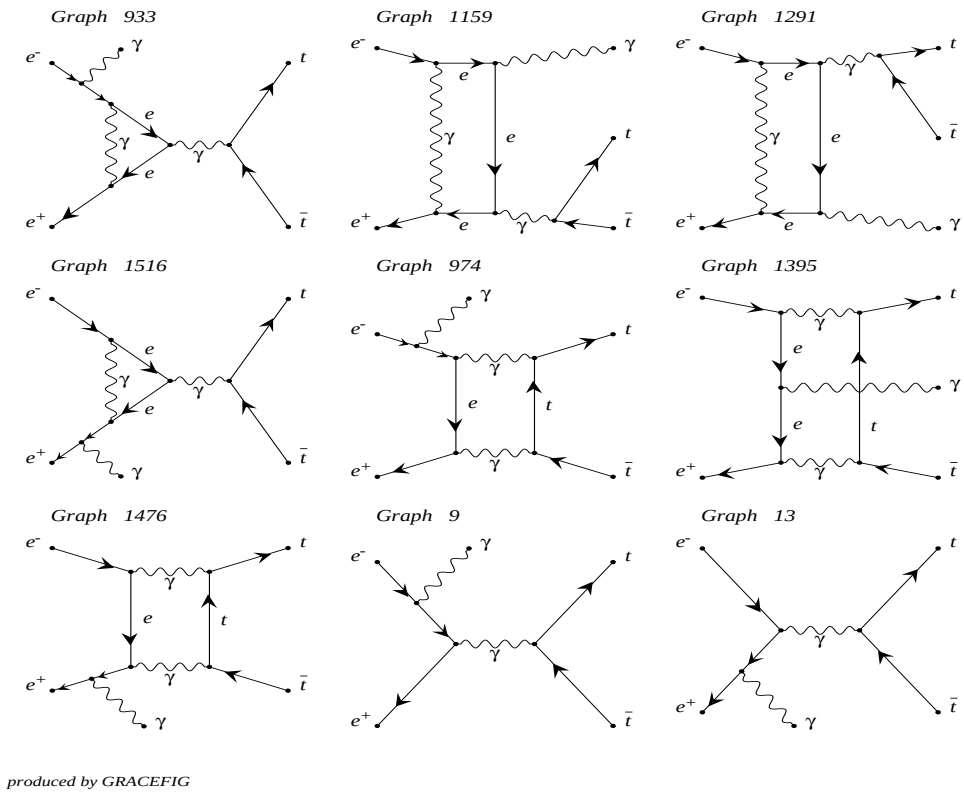

Figure 1: Typical Feynman diagrams as generated by the GRACE-Loop system.

The independence of the result on the five parameters $\tilde{\alpha}, \tilde{\beta}, \tilde{\delta}, \tilde{\kappa}, \tilde{\varepsilon}$ is also checked. The result is presented in table 3. We find that the result is stable over more than 26 digits while varying the non-linear gauge parameters.

Finally, we check the stability of the result versus the soft photon cut parameter (k_c). This test includes both the soft photon and the hard photon contributions. The hard photon bremsstrahlung part is the process $e^+e^- \to t\bar{t}\gamma\gamma$. It is important to note that we have two photons at the final state. One of them has to be applied an energy cut of $E_\gamma^{cut} \geq 10$ GeV and an angle cut of $10^\circ \leq \theta_\gamma^{cut} \leq 170^\circ$. Another one is a hard photon with energy is greater than k_c and smaller than the first photon's energy. This part will be generated by the tree level version of GRACE [32] with the phase space integration by BASES. The result is tested by changing the value of k_c from 10^{-5} GeV to 0.1 GeV. In table 4 we find that the results are in agreement with an accuracy which is better than

C_{UV}	$2\Re(\mathcal{T}^{+}_{Tree}\mathcal{T}_{Loop})$
0	$-5.3131630854021768119477116628317605E^{-3}$
10	$-5.3131630854021768119477116628317726E^{-3}$
100	$-5.3131630854021768119477116628320404E^{-3}$

Table 1: Test of C_{UV} independence of the amplitude. In this table, we take the non-linear gauge parameters to be 0, $\lambda = 10^{-17}$GeV and we use 1 TeV for the center-of-mass energy.

λ [GeV]	$2\Re(\mathcal{T}^{+}_{Tree}\mathcal{T}_{Loop})$+soft contribution
10^{-17}	$-1.6743892369492021873805611201763810E^{-3}$
10^{-19}	$-1.6743892369492020397654354220438766E^{-3}$
10^{-21}	$-1.6743892369492020382892402083349623E^{-3}$

Table 2: Test of the IR finiteness of the amplitude. In this table we take the non-linear gauge parameters to be 0, $C_{UV} = 0$ and the center-of-mass energy is 1 TeV.

0.1% when we vary k_c.

We found that the numerical results are in good agreement when varying C_{UV}, the gauge parameters, photon mass, and k_c. Hereafter, we set $\lambda = 10^{-17}$ GeV, $C_{UV} = 0$ and $\tilde{\alpha} = \tilde{\beta} = \tilde{\delta} = \tilde{\kappa} = \tilde{\varepsilon} = 0$.

3 Results

Our input parameters for the calculation are as follows. The fine structure constant in the Thomson limit is $\alpha^{-1} = 137.0359895$. The mass of the Z boson is $M_Z = 91.187$ GeV. In the on-shell renormalization scheme we take the mass of the W boson (M_W) as an input parameter. It will be derived through the electroweak radiative corrections to the muon decay width (Δr) [33] with $G_\mu = 1.16639 \times 10^{-5}$ GeV^{-2}. Therefore, M_W is a function of M_H. In this calculation, we take $M_H = 120$ GeV and the numerical value of M_W is 80.3759 GeV. For the lepton masses we take $m_e = 0.51099891$ MeV, $m_\tau = 1776.82$ MeV and $m_\mu = 105.658367$ MeV. For the quark masses we take $m_u = 1.7$ MeV, $m_d = 4.1$ MeV, $m_c = 1.27$ GeV, $m_s = 101$ MeV, $m_t = 172.0$ GeV and $m_b = 4.19$ GeV. We apply an energy cut of $E_\gamma^{cut} \geq 10$ GeV and an angle cut of $10^\circ \leq \theta_\gamma^{cut} \leq 170^\circ$ on the photon.

All numerical results are generated by the GRACE-Loop system. For $t\bar{t}$ production the results were first checked with the results in refs [8], [9], [10]. Then we use the values of the parameters above to produce the results of $t\bar{t}$ production in this paper and compare them with $t\bar{t}\gamma$ production.

In Fig 2 the total cross-section is a function of the center-of-mass energy $\sqrt{s}$. We vary the value of $\sqrt{s}$ from 360 GeV to 1 TeV. We find that the cross-section is largest near

$(\tilde{\alpha}, \tilde{\beta}, \tilde{\kappa}, \tilde{\delta}, \tilde{\epsilon})$	$2\Re(\mathcal{T}^{+}_{Tree}\mathcal{T}_{Loop})$
$(0,0,0,0,0)$	$-5.3131630854021768119477116628317605E^{-3}$
$(1,2,3,4,5)$	$-5.3131630854021768119477116637537265E^{-3}$
$(10,20,30,40,50)$	$-5.3131630854021768119477116582762373E^{-3}$

Table 3: Gauge invariance of the amplitude. In this table, we set $C_{UV} = 0$, the photon mass is 10^{-17}GeV and a 1 TeV center-of-mass energy.

k_c[GeV]	σ_H	σ_S	σ_{S+H}
10^{-5}	$4.172723E^{-02}$	$5.885469E^{-02}$	0.10058192
10^{-3}	$2.926684E^{-02}$	$7.131737E^{-02}$	0.10058421
10^{-1}	$1.678994E^{-02}$	$8.377319E^{-02}$	0.10056313

Table 4: Test of the k_c-stability of the result. We choose the photon mass to be 10^{-17} GeV and the center-of-mass energy is 1 TeV. The second column presents the hard photon cross-section and the third column presents the soft photon cross-section. The final column is the sum of both.

the threshold, $\sqrt{s}$ around 550 GeV for $t\bar{t}\gamma$ production and 410 GeV for $t\bar{t}$ production. The total cross-section of $t\bar{t}\gamma$ production is considerably less than 10% of the total cross-section for the $t\bar{t}$ reaction. In addition we find a negative correction for $t\bar{t}\gamma$ production in contrast to the positive correction for $t\bar{t}$ production.

The full $\mathcal{O}(\alpha)$ electroweak corrections take into account the tree graphs and the full one-loop virtual corrections as well as the soft and hard bremsstrahlung contributions. The relative correction is defined as

$$\delta_{EW} = \frac{\sigma(\alpha)}{\sigma_{Tree}} - 1. \tag{2}$$

In order to extract the genuine weak correction in the G_μ scheme, we first evaluate the QED initial radiative correction (δ_{QED}). Applying the structure function method described in ref [34], δ_{QED} is defined as

$$\delta_{QED} = \frac{\sigma_{QED} - \sigma_{Tree}}{\sigma_{Tree}}, \tag{3}$$

with

$$\sigma_{QED}(s) = \int_0^1 dx\ \mathcal{H}(x,s)\ \sigma_0(s(1-x)), \tag{4}$$

here $\mathcal{H}(x,s)$ is a radiator which is defined by formula (11.213) in ref [34]:

$$\mathcal{H}(x,s) = \Delta\beta x^{\beta-1} - \beta(1-\frac{x}{2})$$

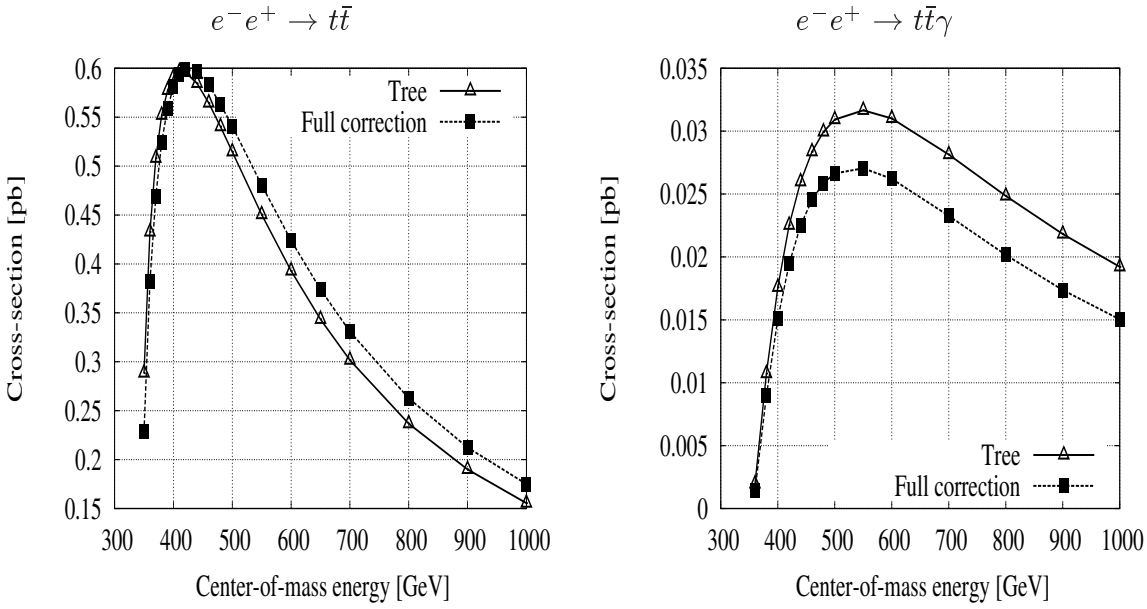

Figure 2: The total cross-section as a function of center-of-mass energy. The left figure is the result of $t\bar{t}$ production and the right figure shows the result of the $t\bar{t}\gamma$ reaction. The triangle points are the result of the tree level calculation while the rectangular points are the sum of the tree level calculation combined with the full one-loop electroweak radiative corrections. Lines are only guide for the eyes.

$$+ \quad \frac{\beta^2}{8}\Big[-4(2-x)\ln x - \frac{1+3(1-x)^2}{x}\ln(1-x) - 6 + x\Big] \tag{5}$$

with $\beta = \frac{2\alpha}{\pi}\Big(\ln(\frac{s}{m_e^2}) - 1\Big)$ and $\Delta = 1 + \frac{\alpha}{\pi}\Big(\frac{3}{2}\ln(\frac{s}{m_e^2}) + \frac{\pi^2}{3} - 2\Big)$.

After obtaining the QED correction, we define the genuine weak correction in the α scheme:

$$\delta_W = \delta_{EW} - \delta_{QED}. \tag{6}$$

Having subtracted the genuine weak correction in the α scheme, one can express the correction in the G_μ scheme. Next we subtract the universal weak correction which is obtained from Δr. The genuine weak correction in the G_μ scheme is defined by

$$\delta_W^{G_\mu} = \delta_W - n\Delta r, \tag{7}$$

with $\Delta r = 2.55\%$ for $M_H = 120$ GeV and $n = 3(2)$ for $t\bar{t}\gamma$ (for $t\bar{t}$) production respectively.

In Fig 3, we present the full electroweak correction and the genuine weak correction in both the α and the G_μ schemes for $t\bar{t}\gamma$ production as compared to $t\bar{t}$ production. These corrections are shown as a function of the center-of-mass energy, $\sqrt{s}$. We vary $\sqrt{s}$ from 360 GeV to 1 TeV. The figures show clearly that the QED correction is dominant in the low energy region. In the high energy region it is much smaller ($\sim -5\%$ at 1 TeV). In contrast to the QED correction the weak correction in the α scheme is less than 10% for low energies but reaches -16% at 1 TeV center-of-mass energy. For $t\bar{t}\gamma$ production, we find that the value of the genuine weak correction in the G_μ scheme varies from 2% to -24% over $\sqrt{s}$ from 360 GeV to 1 TeV.

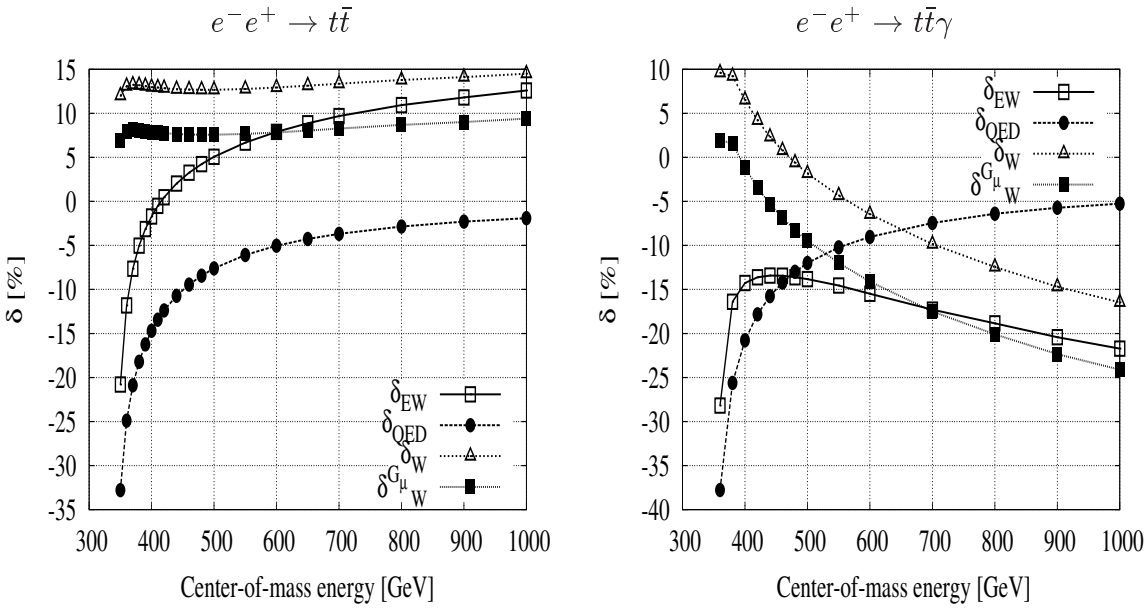

Figure 3: The full electroweak correction and the genuine weak correction as a function of the center-of-mass energy. The left figure shows the results for $t\bar{t}$ production while the right figure shows the results for $t\bar{t}\gamma$ production. The circle points represent the QED correction, the empty rectangle points are the results for the full electroweak correction while the triangle points are the results for the genuine weak correction in the α scheme. The filled rectangle points represent the results of the genuine weak correction in the G_μ scheme. Lines are only guide for the eyes.

Now we turn our attention to the forward-backward asymmetry A_{FB}. This quantity is defined as

$$A_{FB} = \frac{\sigma(0^\circ \leq \theta_t \leq 90^\circ) - \sigma(90^\circ \leq \theta_t \leq 180^\circ)}{\sigma(0^\circ \leq \theta_t \leq 90^\circ) + \sigma(90^\circ \leq \theta_t \leq 180^\circ)}, \tag{8}$$

with θ_t the angle of the top quark.

Fig 4 shows the results for A_{FB} as a function of the center-of-mass energy. The figures show clearly that the top quark asymmetry in the full results is smaller than the asymmetry at the tree level results only.

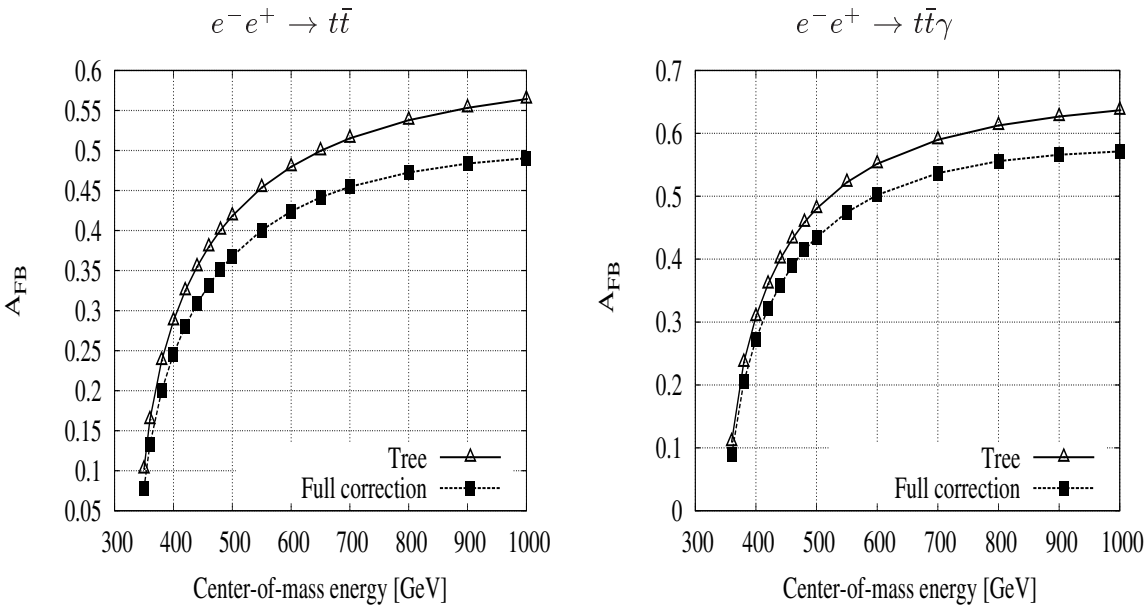

Figure 4: The top quark forward-backward asymmetry as a function of the center-of-mass energy. Left figure is the results for $t\bar{t}$ production and right one is the results for $t\bar{t}\gamma$ production. The triangle points represent the tree level results and the rectangle points are the results including the full radiative corrections. Lines are only guide for the eyes.

In Fig 5 we compare the values of A_{FB} in $t\bar{t}\gamma$ production directly with its value for $t\bar{t}$ production. From the figures, we find that A_{FB} in $t\bar{t}\gamma$ production is larger than A_{FB} in $t\bar{t}$ production. This is the most important result of the paper. The effect should be clearly observable at the ILC.

4 Conclusions

We have presented the full $\mathcal{O}(\alpha)$ electroweak radiative corrections to the process $e^+e^- \to t\bar{t}\gamma$ and $e^+e^- \to t\bar{t}$ at ILC. The calculations were done with the help of the GRACE-Loop system.

GRACE-Loop have implemented a generalised non-linear gauge fixing condition which includes five gauge parameters. With the UV, IR finiteness and gauge parameters inde-

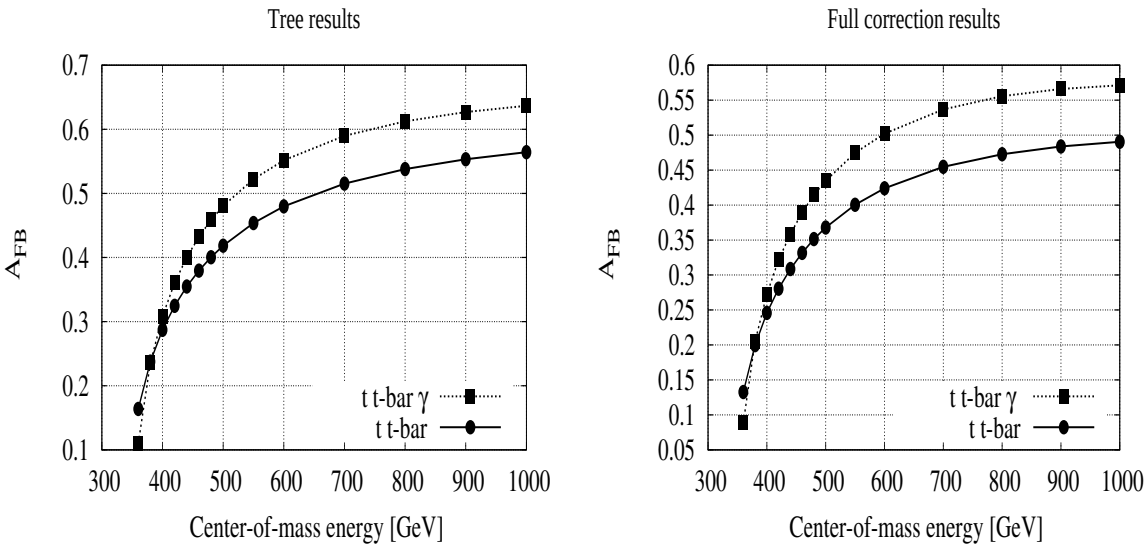

Figure 5: The value of the top quark asymmetry in $t\bar{t}\gamma$ production as compared to $t\bar{t}$ production. The rectangular points (circle points) represent the result for $t\bar{t}\gamma$ production ($t\bar{t}$ production) respectively. Lines are only guide for the eyes.

pendence checks, the system provide a powerful tool to test the results in the consistency way. In the numerical checks of this calculation, we find that the results are numerically stable when quadruple precision is used.

We find that the numerical value of the genuine weak corrections in G_μ scheme varies from 2% to -24% in the range of center-of-mass energy from 360 GeV to 1TeV. We also obtain a large value for the top quark forward-backward asymmetry in the $t\bar{t}\gamma$ process as compared with the one in $t\bar{t}$ production.

We also introduce the axial gauge for the external photon in the GRACE-Loop system. It helps to avoid a large numerical cancellation problem. This is very useful when calculating Bhabha scattering at small angle and energy cuts of the final state particles. Bhabha scattering and related processes are not only used as luminosity monitor, but also play an important role as backgrounds for the process $e^-e^+ \to \tilde{\chi}^-\tilde{\chi}^+\gamma$, which is a very interesting reaction for the search for dark matter. We will address it in a future publication.

In addition, this calculation will provide a framework for calculating the full $\mathcal{O}(\alpha)$ electroweak radiative corrections for the process $e^+e^- \to e^+e^-\gamma$. This reaction and these corrections will play an important role at future e^+e^- colliders like the ILC.

Acknowledgments

We wish to thank Dr. F. Yuasa and Dr. N. Watanabe for valuable discussions and comments. This work was supported by JSPS KAKENHI Grant Number 20340063. The work of T.U. was supported by the DFG through SFB/TR 9 "Computational Particle Physics".

References

[1] T. Aaltonen *et al.* [CDF Collaboration], Phys. Rev. D **83**, 112003 (2011) [arXiv:1101.0034 [hep-ex]].

[2] V. M. Abazov *et al.* [D0 Collaboration], Phys. Rev. Lett. **100**, 142002 (2008) [arXiv:0712.0851 [hep-ex]].

[3] A. Denner, S. Dittmaier, S. Kallweit and S. Pozzorini, Phys. Rev. Lett. **106** (2011) 052001 [arXiv:1012.3975 [hep-ph]].

[4] A. Denner, S. Dittmaier, S. Kallweit and S. Pozzorini, JHEP **1210** (2012) 110 [arXiv:1207.5018 [hep-ph]].

[5] G. Bevilacqua, M. Czakon, A. van Hameren, C. G. Papadopoulos and M. Worek, JHEP **1102** (2011) 083 [arXiv:1012.4230 [hep-ph]].

[6] K. Melnikov, M. Schulze and A. Scharf, Phys. Rev. D **83** (2011) 074013 [arXiv:1102.1967 [hep-ph]].

[7] K. Melnikov, A. Scharf and M. Schulze, Phys. Rev. D **85** (2012) 054002 [arXiv:1111.4991 [hep-ph]].

[8] J. Fujimoto and Y. Shimizu, Mod. Phys. Lett. **3A**, 581 (1988).

[9] J. Fleischer, T. Hahn, W. Hollik, T. Riemann, C. Schappacher and A. Werthenbach, hep-ph/0202109.

[10] J. Fleischer, A. Leike, T. Riemann and A. Werthenbach, Eur. Phys. J. C **31**, 37 (2003) [hep-ph/0302259].

[11] G. Aad *et al.* [ATLAS Collaboration], Phys. Lett. B **716** (2012) 1 [arXiv:1207.7214 [hep-ex]].

[12] S. Chatrchyan *et al.* [CMS Collaboration], Phys. Lett. B **716** (2012) 30 [arXiv:1207.7235 [hep-ex]].

[13] J. Fleischer, F. Jegerlehner and M. Zralek, Z. Phys. C **42** (1989) 409.

[14] K. Aoki, Z. Hioki, R. Kawabe, M. Konuma and T. Muta, Suppl. Prog. Theor. Phys. **73** (1982) 1.

[15] G. Belanger, F. Boudjema, J. Fujimoto, T. Ishikawa, T. Kaneko, K. Kato and Y. Shimizu, Phys. Rept. **430**, 117 (2006) [hep-ph/0308080].

[16] G. Belanger, F. Boudjema, J. Fujimoto, T. Ishikawa, T. Kaneko, Y. Kurihara, K. Kato and Y. Shimizu, Phys. Lett. B **576** (2003) 152 [hep-ph/0309010].

[17] G. Belanger, F. Boudjema, J. Fujimoto, T. Ishikawa, T. Kaneko, K. Kato, Y. Shimizu and Y. Yasui, Phys. Lett. B **571**, 163 (2003) [hep-ph/0307029].

[18] G. Belanger, F. Boudjema, J. Fujimoto, T. Ishikawa, T. Kaneko, K. Kato and Y. Shimizu, Nucl. Phys. Proc. Suppl. **116**, 353 (2003) [hep-ph/0211268].

[19] R. -Y. Zhang, W. -G. Ma, H. Chen, Y. -B. Sun and H. -S. Hou, Phys. Lett. B **578** (2004) 349 [hep-ph/0308203].

[20] Y. You, W. -G. Ma, H. Chen, R. -Y. Zhang, S. Yan-Bin and H. -S. Hou, Phys. Lett. B **571** (2003) 85 [hep-ph/0306036].

[21] A. Denner, S. Dittmaier, M. Roth and M. M. Weber, Phys. Lett. B **575** (2003) 290 [hep-ph/0307193].

[22] A. Denner, S. Dittmaier, M. Roth and M. M. Weber, Nucl. Phys. B **680** (2004) 85 [hep-ph/0309274].

[23] A. Denner, S. Dittmaier, M. Roth and M. M. Weber, Phys. Lett. B **560** (2003) 196 [hep-ph/0301189].

[24] A. Denner, S. Dittmaier, M. Roth and M. M. Weber, Nucl. Phys. B **660** (2003) 289 [hep-ph/0302198].

[25] K. Kato, F. Boudjema, J. Fujimoto, T. Ishikawa, T. Kaneko, Y. Kurihara, Y. Shimizu and Y. Yasui, PoS HEP **2005** (2006) 312.

[26] J. A. M. Vermaseren:*New Features of FORM*; math-ph/0010025.

[27] A.C. Hearn: *REDUCE User's Manual*, version 3.7, Rand. Corp. 1999.

[28] G. J. van Oldenborgh, *Comput. Phys. Commun.* **58** (1991) 1.

[29] T. Hahn, `LoopTools`, `http://www.feynarts.de/looptools/`.

[30] S. Kawabata, *Comp. Phys. Commun.* **41** (1986) 127; *ibid.,* **88** (1995) 309.

[31] F. Boudjema and E. Chopin, *Z. Phys.* **C73** (1996) 85; hep-ph/9507396.

[32] T. Ishikawa, T. Kaneko, K. Kato, S. Kawabata, Y. Shimizu and H. Tanaka, KEK Report 92-19, 1993, `GRACE` manual Ver. 1.0.

[33] Z. Hioki, Acta Phys. Polon. B **27**, 2573 (1996) [hep-ph/9510269].

[34] J. Fujimoto, M. Igarashi, N. Nakazawa, Y. Shimizu and K. Tobimatsu, *Suppl. Prog. Theor. Phys.* **100** (1990) 1.